Dominant and recessive deafness caused by mutations of a novel gene, *TMC1*, required for cochlear hair-cell function

Kiyoto Kurima[1], Linda M. Peters[2], Yandan Yang[1], Saima Riazuddin[2], Zubair M. Ahmed[2,3], Sadaf Naz[2], Deidre Arnaud[4], Stacy Drury[4], Jianhong Mo[2], Tomoko Makishima[1], Manju Ghosh[5], P.S.N. Menon[5], Dilip Deshmukh[6], Carole Oddoux[7], Harry Ostrer[7], Shaheen Khan[3], Sheikh Riazuddin[3], Prescott L. Deininger[8], Lori L. Hampton[9], Susan L. Sullivan[10], James F. Battey, Jr.[9], Bronya J.B. Keats[4], Edward R. Wilcox[2], Thomas B. Friedman[2] & Andrew J. Griffith[1,11]

Published online: 19 February 2002, DOI: 10.1038/ng842

Positional cloning of hereditary deafness genes is a direct approach to identify molecules and mechanisms underlying auditory function. Here we report a locus for dominant deafness, DFNA36, which maps to human chromosome 9q13–21 in a region overlapping the DFNB7/B11 locus for recessive deafness. We identified eight mutations in a new gene, transmembrane cochlear-expressed gene 1 (*TMC1*), in a DFNA36 family and eleven DFNB7/B11 families. We detected a 1.6-kb genomic deletion encompassing exon 14 of *Tmc1* in the recessive deafness (*dn*) mouse mutant, which lacks auditory responses and has hair-cell degeneration[1,2]. *TMC1* and *TMC2* on chromosome 20p13 are members of a gene family predicted to encode transmembrane proteins. *Tmc1* mRNA is expressed in hair cells of the postnatal mouse cochlea and vestibular end organs and is required for normal function of cochlear hair cells.

Introduction

Molecules underlying transduction of visual, olfactory, gustatory and touch stimuli have been identified in mammals, yet the molecular bases of many of the most basic auditory system phenomena remain unknown[3]. Functional and cDNA cloning of genes that are important for auditory function is hindered by the scarce amounts of neurosensory tissue in the inner ear. Positional cloning of genes underlying human and mouse forms of hereditary deafness circumvents these limitations and can identify molecular substrata responsible for perception and processing of sound in the auditory system[4]. Genes identified through human and mouse models of hereditary deafness have begun to define crucial molecules in the inner ear underlying its morphogenesis, specialized extracellular matrices, the development, structure and function of neurosensory hair cells, and electrochemical homeostasis. In spite of this rapid progress, genetic dissection of the auditory system is incomplete[5]. Positional cloning of hereditary hearing-loss genes continues to identify new molecules and mechanisms underlying both normal and pathologic processes in the auditory system[6–11].

We report here the identification of *TMC1*, which underlies dominant and recessive nonsyndromic hearing loss at the DFNA36 and DFNB7/B11 loci. *TMC1* is one member of a new family of genes encoding transmembrane proteins of unknown function. We also describe the mouse ortholog, *Tmc1*, and show that it is mutated in the recessive deafness (*dn*) mutant. The auditory phenotype of *dn* mutant mice[1,2] suggests a possible role for *TMC1* in mechanoelectrical transduction of sound by cochlear hair cells.

Results

Genetic map of DFNA36 and DFNB7/B11

We ascertained a large North American family, LMG128 (Fig. 1*a*), segregating dominant, nonsyndromic, bilateral, symmetric, sensorineural hearing loss that begins at 5–10 years of age and rapidly progresses to profound deafness within 10–15 years (Fig. 1*b*). Affected individuals had no evidence of vestibular deficits in their developmental and medical histories or upon physical examination. The hearing-loss phenotype did not segregate with microsatellite markers flanking any of the known DFNA loci,

[1]*Section on Gene Structure and Function and* [2]*Section on Human Genetics, Laboratory of Molecular Genetics, National Institute on Deafness and Other Communication Disorders, National Institutes of Health, 5 Research Court, Rockville, Maryland 20850, USA.* [3]*Center of Excellence in Molecular Biology, Punjab University, Thokar Niaz Baig, Lahore, Pakistan.* [4]*Department of Genetics, Louisiana State University Health Sciences Center, New Orleans, Louisiana, USA.* [5]*Genetics Unit, Department of Pediatrics, All India Institute of Medical Sciences, New Delhi, India.* [6]*Rotary Deaf School, Ichalkaranji-Tilawani, Maharashtra, India.* [7]*Human Genetics Program, Department of Pediatrics, New York University School of Medicine, New York, New York, USA.* [8]*Department of Environmental Health Sciences, Tulane University Medical Center, New Orleans, Louisiana, USA.* [9]*G-protein Coupled Receptors' Section, National Institute of Neurological Disorders and Stroke, National Institutes of Health, 50 Center Drive, Bethesda, Maryland, USA.* [10]*Section on Molecular Neuroscience and* [11]*Hearing Section, National Institute on Deafness and Other Communication Disorders, National Institutes of Health, 5 Research Court, Rockville, Maryland 20850, USA. Correspondence should be addressed to A.J.G. (e-mail: griffita@nidcd.nih.gov).*

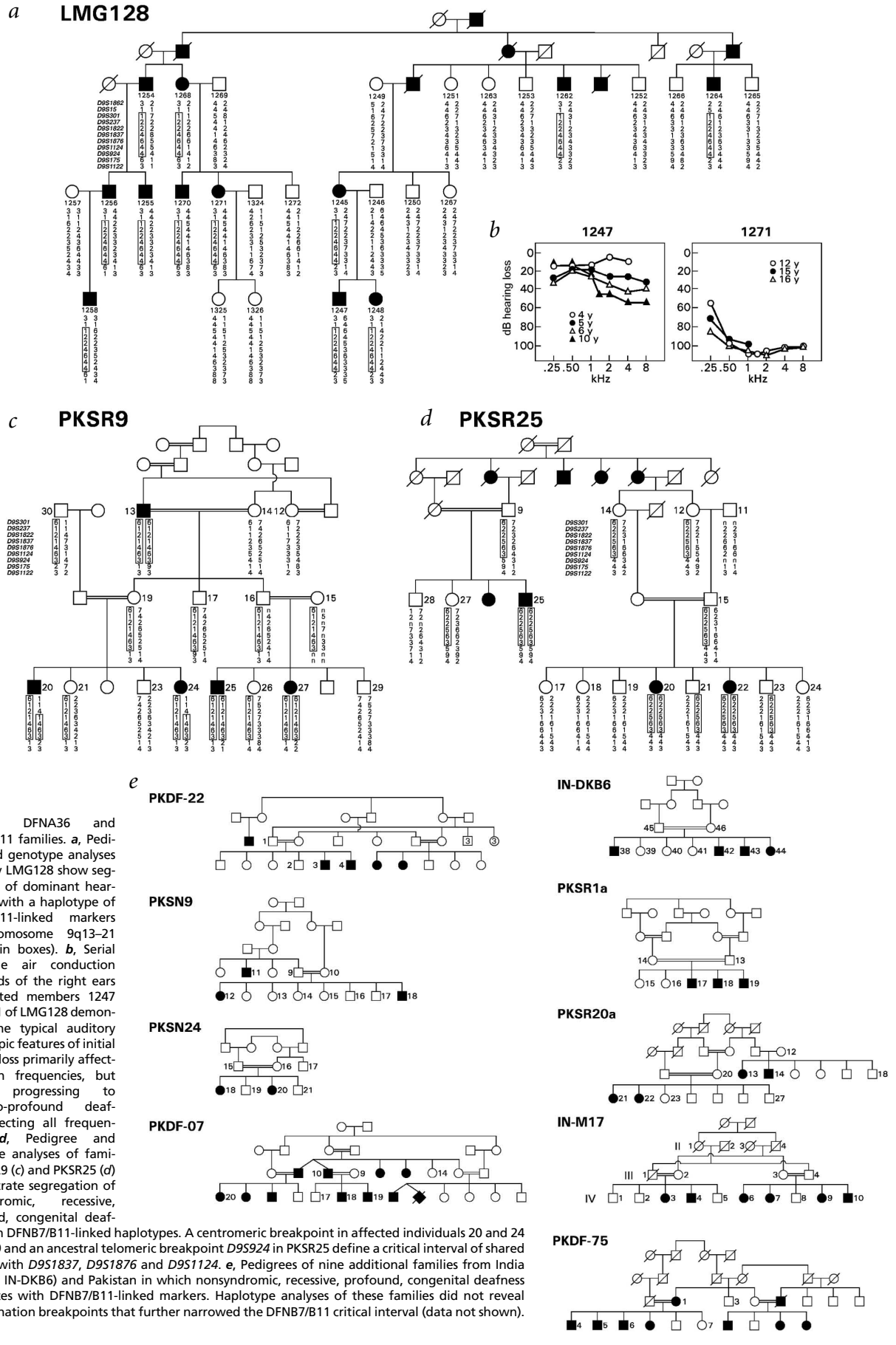

Fig. 1 DFNA36 and DFNB7/B11 families. ***a***, Pedigree and genotype analyses of family LMG128 show segregation of dominant hearing loss with a haplotype of DFNB7/B11-linked markers on chromosome 9q13–21 (shown in boxes). ***b***, Serial pure-tone air conduction thresholds of the right ears of affected members 1247 and 1271 of LMG128 demonstrate the typical auditory phenotypic features of initial hearing loss primarily affecting high frequencies, but rapidly progressing to severe-to-profound deafness affecting all frequencies. ***c,d***, Pedigree and genotype analyses of families PKSR9 (*c*) and PKSR25 (*d*) demonstrate segregation of nonsyndromic, recessive, profound, congenital deafness with DFNB7/B11-linked haplotypes. A centromeric breakpoint in affected individuals 20 and 24 of PKSR9 and an ancestral telomeric breakpoint *D9S924* in PKSR25 define a critical interval of shared linkage with *D9S1837*, *D9S1876* and *D9S1124*. ***e***, Pedigrees of nine additional families from India (IN-M17, IN-DKB6) and Pakistan in which nonsyndromic, recessive, profound, congenital deafness segregates with DFNB7/B11-linked markers. Haplotype analyses of these families did not reveal recombination breakpoints that further narrowed the DFNB7/B11 critical interval (data not shown).

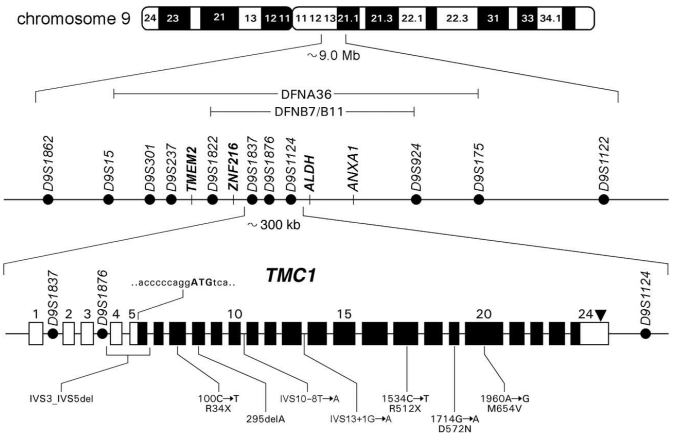

Fig. 2 Physical map of the DFNA36/B7/B11 region defined by critical recombinations in families LMG128, PKSR9 and PKSR25. The schematic illustration of the genomic structure of *TMC1* indicates a probable translation initiation codon sequence, exon numbers, a polyadenylation signal sequence (black triangle) and DFNA36 and DFNB7/B11 mutations.

indicating that it defined a new nonsyndromic dominant deafness locus. Genotype analysis of markers linked to known nonsyndromic recessive deafness (DFNB) loci revealed linkage of DFNA36 to markers spanning the previously mapped DFNB7/B11 interval on chromosome 9q13–21 (lod=6.31 for *D9S1124* at θ=0; Figs 1*a* and 2)[12,13].

Deafness in DFNA36 and DFNB7/B11 families was therefore potentially caused by mutations of the same gene. Approximately 230 consanguineous Indian and Pakistani families with three or more affected individuals segregating nonsyndromic recessive deafness were screened for linkage to markers in the DFNA36 and DFNB7/B11 critical intervals on chromosome 9q13–21. In addition to the original DFNB7 family IN-M17 (ref. 12), ten unreported DFNB7/B11 families were ascertained (Fig. 1*c*,*d*,*e*). Haplotype analyses of chromosome 9q13–21 markers in these families showed a small region of shared linkage between *D9S1822* and *D9S924* (Fig. 2), defined by a centromeric recombination breakpoint in individuals 20 and 24 of PKSR9 (Fig. 1*c*) and an ancestral telomeric breakpoint in PKSR25 (Fig. 1*d*). The combined critical interval of approximately 3 Mb narrowed both ends of a previously reported region for this locus[14] and is entirely contained within the 6-Mb critical interval for DFNA36 between *D9S15* and *D9S175* (Fig. 2).

We evaluated positional candidate genes in the DFNA36 and DFNB7/B11 critical regions by sequence analysis of predicted exons in genomic DNA from affected individuals from the DFNA36 family and the 11 DFNB7/B11 families. We did not find mutations in the *TMEM2*, *ZNF216*, *ALDH1A1* or *ANXA1* genes (Fig. 2). BLASTx, GENSCAN and FGENES analyses identified one predicted gene (with sequence similarity to the expressed-sequence tag KIAA1099) in the critical region, but no mutations were detected (data not shown).

The *TMC* gene family

To identify additional DFNA36/B7/B11 candidate genes based upon sequence similarity to related genes elsewhere in the genome, we initiated a systematic tBLASTx analysis of segments of genomic DNA sequence in the DFNA36/B7/B11 interval. Query sequences from BAC 296H15 containing part of this interval were similar to a predicted gene (subsequently named *TMC2*) on chromosome 20p13. We used conserved sequences between *TMC2* and the query sequence (subsequently named *TMC1*) on chromosome 9q13–21 to design primers for amplifying potential *TMC1* transcripts from a human fetal-brain cDNA library. We sequenced a 0.8-kb amplification product and confirmed that it represented an mRNA transcript corresponding to exons 7–16 of

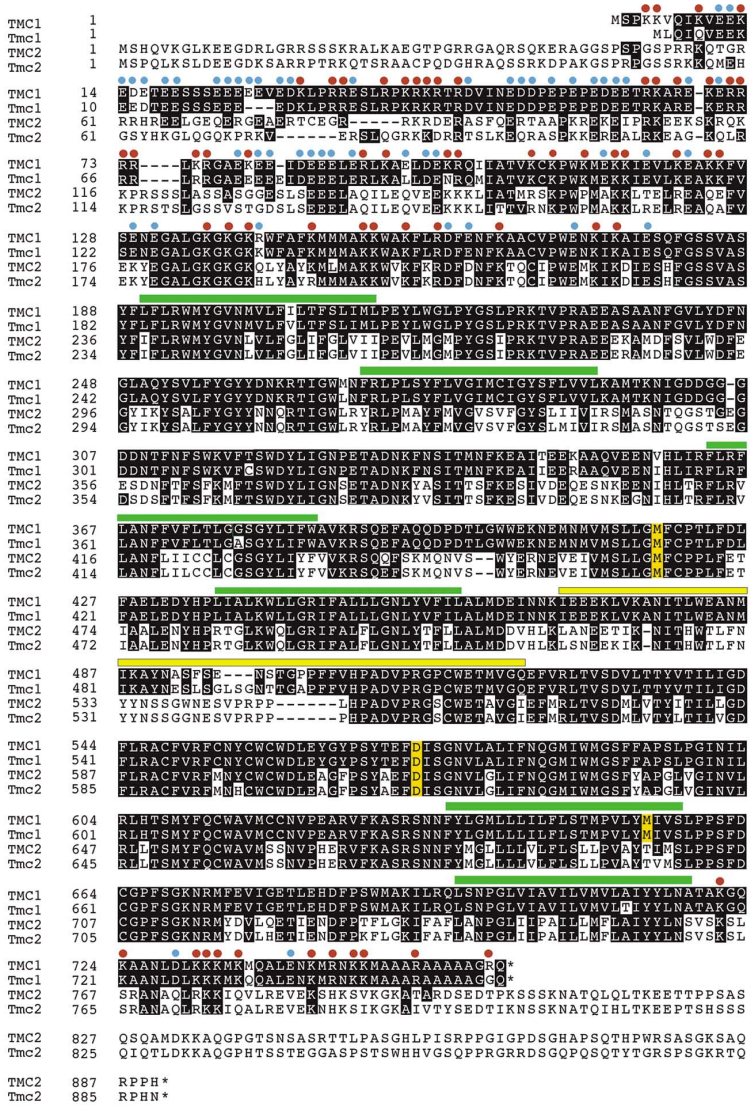

Fig. 3 Clustal W alignment of deduced amino-acid sequences of *TMC1*, *Tmc1*, *TMC2* and *Tmc2* (ref. 17). The shared amino-acid sequence identity of *TMC1* with at least one of the other three genes is indicated by shaded boxes. Dashes (–) indicate sequence gaps, green bars indicate regions of *TMC1* predicted to be transmembrane domains by TMHMM2.0, and the yellow bar indicates the 57 amino acids of *Tmc1* deleted in *dn* mice. Red dots indicate positively charged amino-acid residues, and blue dots indicate negatively charged residues in the N- and C-terminal domains. Residues substituted by missense mutations in Beethoven (ref. 25; M412), LMG128 (D572) and IN-M17 (M654) are highlighted in orange boxes.

TMC1 (Fig. 2). 5′ and 3′ RACE of human inner-ear cDNA produced additional cDNA fragments whose aligned sequences included a (longest) open reading frame (ORF) of 2,283 nt, predicted to encode an 87-kD protein. Alignment of the cDNA with genomic sequences showed that 24 exons probably encode the full-length mRNA, including 4 exons encoding sequence upstream of a methionine codon in exon 5 (Fig. 2). There are many in-frame stop codons directly upstream of this methionine codon, which is predicted to be an adequate Kozak translation initiation codon (Fig. 2)[15].

We obtained the orthologous mouse *Tmc1* cDNA by RT–PCR and 5′ and 3′ RACE of mouse inner-ear cDNA. Overlapping cDNA products were aligned to identify the longest (2,274 nt) ORF of mouse *Tmc1*, which is also predicted to encode an 87-kD protein. The putative translation initiation codon is also preceded by an in-frame, upstream stop codon. The adjacent sequence, tcttttATGt, does not have a purine at –3 or guanine at +4, which are the two most conserved positions of the consensus translation-initiation sequence[15,16]. The next in-frame methionine codon is at M107, which corresponds to M113 in human TMC1 and has the conserved purine at –3 and guanine at +4. The genomic structure of *Tmc1* was determined by aligning cDNA sequence with mouse genomic DNA sequence. The *Tmc1* ORF is encoded by 20 exons, with one upstream exon encoding the 5′ untranslated region (UTR; data not shown).

We determined the cDNA and genomic nucleotide sequences of *TMC2* and *Tmc2* by aligning sequences of RT–PCR and RACE products obtained from inner ear, brain and testis tissues. *TMC2* and *Tmc2* are predicted to encode 101-kD polypeptides whose sequence divergence with *TMC1* and *Tmc1* occurs mainly in the amino and carboxy termini of the proteins. Comparison of the amino-acid sequences of full-length TMC2 and Tmc2 reveals 83% identity, 57% identity of human TMC1 and TMC2, and 58% identity of mouse Tmc1 and Tmc2 (Fig. 3)[17].

TMC1 mutations in DFNA36 and DFNB7/B11 deafness

Nucleotide-sequence analysis of *TMC1* genomic DNA from affected members of family LMG128 (Fig. 1*a*) identified a 1714G→A transition predicted to result in a substitution of asparagine for aspartic acid at amino-acid position 572 (Fig. 4*a*). This aspartic acid is conserved in *TMC1*, *Tmc1*, *TMC2* and *Tmc2*. Sequence analysis of 283 ethnically matched control DNA samples, 68 control samples from a panethnic human diversity panel, and 100 samples from a Caucasian diversity panel revealed that 0 of 902 chromosomes contained this substitution.

Pathogenic *TMC1* mutations were identified in ten DFNB7/B11 families, including two nonsense mutations, 100C→T (R34X) and 1534C→T (R512X), 295delA which results in a frameshift and premature termination, and a point mutation 1960A→G predicted to substitute valine for a conserved methionine at position 654 (Fig. 4*e*). We identified 100C→T (R34X) in five different families from Pakistan. Comparison of the linked haplotypes at *D9S1124*, *D9S1837* and *D9S1876* in these families with those in Pakistani individuals with normal hearing (controls) confirmed a specific association of R34X with a single identical haplotype of these markers (data not shown). The R34X mutation in these apparently unrelated families was probably derived from a common founder, although it is possible that it is a recurrent mutation on this haplotype.

Exons 4 and 5 could not be amplified from affected members of family PKDF22. Sequence analysis of genomic DNA amplified with more distant flanking primers revealed a homozygous genomic 26.7-kb deletion of exons 4 and 5 (IVS3_IVS5del27kb) in deaf PKDF22 family members (Fig. 4*f*). Other mutations of *TMC1* included an IVS13+1G→A transition in a splice donor site in family PKSR1a (Fig. 4*g*). These two mutations, together with the other four mutations, thus accounted for deafness in 10 of the 11 DFNB7/B11 families. The eleventh DFNB7/B11 family, PKSR25, segregated an IVS10–8T→A transversion in a splice-acceptor site (Fig. 4*h*); however, the pathogenic effect of this change is unknown.

Analyses of *TMC1* sequence in remaining family members confirmed complete penetrance and co-segregation of these mutations with DFNB7/B11-linked deafness in all of the families. We did not detect any of the DFNB7/B11 mutations in ethnically matched (Pakistani or Indian), normal-hearing control

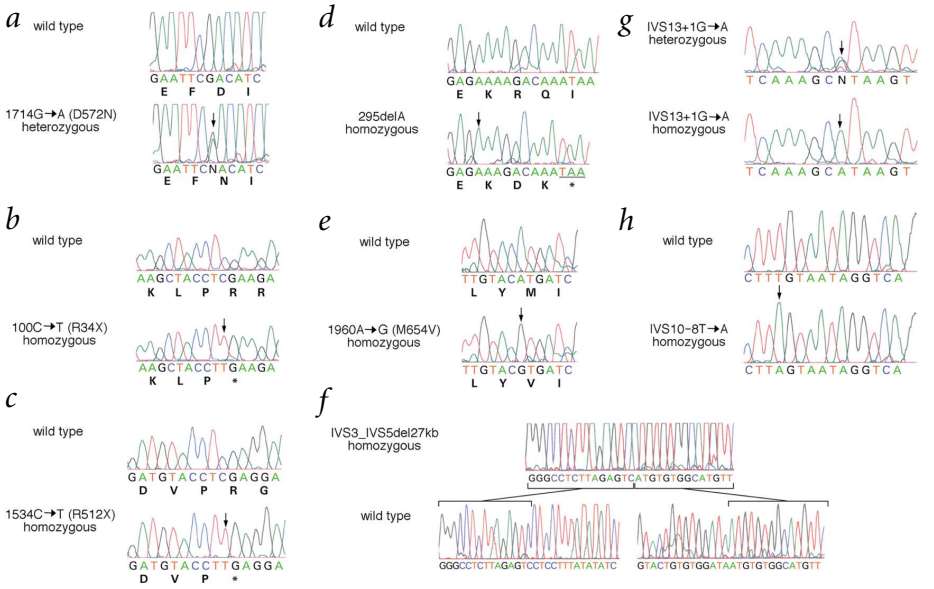

Fig. 4 *TMC1* mutations segregating in DFNA36 and DFNB7/B11 families. ***a***, Heterozygous 1714G→A (D572N) missense substitution in affected individual 1256 of family LMG128 segregating dominant DFNA36 hearing loss. Wildtype sequence for unaffected family member 1265 is shown for comparison. ***b***, Representative electropherogram from affected individual 20 of family PKSR9 showing the homozygous 100C→T (R34X) nonsense mutation observed to segregate with DFNB7/B11 deafness in families PKSR9, PKSN9, PKSN24, PKDF7 and PKDF75. Corresponding wildtype sequence is shown for unaffected PKSR9 family member 23. ***c***, Homozygous 1534C→T (R512X) nonsense mutation in affected individual 21 and wildtype sequence in unaffected member 23 of family PKSR20a. ***d***, Homozygous 295delA frameshift mutation predicted to cause premature translation termination in affected individual 43 of family IN-DKB6, compared with wildtype sequence shown for family member 39. ***e***, Homozygous 1960A→G (M654V) missense substitution in affected individual IV-9 and wildtype sequence from unaffected member IV-1 of family IN-M17. ***f***, Electropherogram from affected individual of family PKDF22 shows the deletion breakpoints in IVS3 and IVS5, corresponding to the homozygous deletion of 26,728 bp of genomic DNA including exons 4 and 5 (IVS3_IVS5del27kb). ***g***, Homozygous and heterozygous IVS13+1G→A mutations affecting a splice-donor site in deaf individual 17 and his unaffected sibling (15) in family PKSR1a. ***h***, Homozygous and wildtype IVS10–8T→A point mutations in a splice-acceptor site in affected individual 20 and her unaffected sibling (24) in family PKSR25.

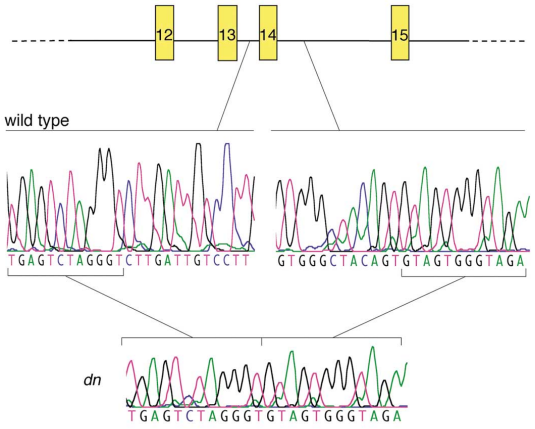

Fig. 5 Intragenic deletion of exon 14 of *Tmc1* in deafness (*dn*) mice. Schematic illustration of the genomic structure of *Tmc1* and the IVS13_IVS14del1.6kb mutation in *dn* mice, with nucleotide sequences for deafness and wildtype parental strain (*ct*) mice across the IVS13_IVS14del1.6kb breakpoints.

DNA samples (n=83–96) or in samples from a panethnic Human Diversity Panel (n=77–88), consistent with the pathogenic roles of these mutations in DFNB7/B11 deafness.

Mouse deafness is a recessive allele of *Tmc1*

We previously proposed the recessive deafness (*dn*) locus on mouse chromosome 19 as a candidate model for recessive DFNB7 deafness in humans[12]. The integrated genetic and physical maps of this region confirmed that *Tmc1* lies within the *dn* critical interval[18]. PCR analysis of *Tmc1* failed to amplify any products from *dn/dn* genomic DNA with primers flanking exons 13 or 14. Amplification and sequence analysis of all other *Tmc1* exons revealed no differences between *dn/dn* and parental strain DNA. The pattern and sizes of products obtained with nested primer pairs were consistent with a 1.6-kb deletion in *dn* genomic DNA (data not shown). Sequence analysis of these amplification products identified a 1,656-bp deletion encompassing the 171-bp exon 14 and the adjacent regions of introns 13 and 14 (Fig. 5), including the reverse-priming site for amplification of exon 13. This result was confirmed by Southern-blot analysis (data not shown). The splice sites for exons 13 and 15 are not deleted, and nucleotide sequence analysis of $Tmc1^{dn}$ cDNA confirmed that IVS13_IVS14del1.6kb causes an in-frame deletion of exon 14 from *Tmc1* mRNA. Nucleotide sequence analysis of cDNA fragments spanning the rest of the full-length $Tmc1^{dn}$ mRNA detected no other differences from wildtype *Tmc1*. Real-time quantitative RT–PCR analysis of RNA from brain and testis revealed approximately similar *Tmc1* mRNA levels in $Tmc1^{dn/dn}$ and $Tmc1^{ct/ct}$ control mice (data not shown). IVS13_IVS14del1.6kb was not observed in DNA from the parental strain or 13 other diverse mouse strains, providing additional evidence of the pathogenic role of this mutation in deafness mice.

Predicted structural motifs of TMC1

Using BLAST and PROSITE analyses of *TMC1*, we found no significant sequence similarities to characterized genes or motifs that might provide insight into the putative function of *TMC1*. TMHMM2.0 analysis predicted six transmembrane domains with a cytoplasmic orientation of the N and C termini[19]. These regions predicted by TMHMM2.0 correspond to those predicted by TMpred to have the highest probability of being transmembrane helices; TMHMM2.0 has been reported to be more sensitive and specific for detection of transmembrane regions[19]. Analysis of TMC1 and Tmc1 with the SignalP v. 2.0 algorithm detected no signal-peptide sequences[20].

The N termini of TMC1 and Tmc1 are predicted to have a high proportion of charged amino-acid residues (66/99 and 59/93, respectively) that are grouped together in alternating clusters of approximately 9–12 residues of identical charge (Fig. 3). The next 80 amino acids have a lower, but significant, proportion of charged side chains (29/80), and the C terminus also has numerous positively charged side chains. These regions of TMC1 and Tmc1 have no detectable sequence similarity to known proteins or structural motifs.

Tissue-specific expression of *TMC* and *Tmc* mRNA

RT–PCR analyses detected *TMC1*, *Tmc1*, *TMC2* and *Tmc2* mRNA transcripts in human fetal cochlea and inner-ear tissue of postnatal mouse. Northern-blot analysis with a cDNA probe for the 3′ UTR of *TMC1* revealed weak hybridization to RNA from human placenta and testis but not other tissues. A northern blot of RNA from a variety of mouse tissues probed with the 3′ UTR of *Tmc1* confirmed hybridization to an RNA species of approximately

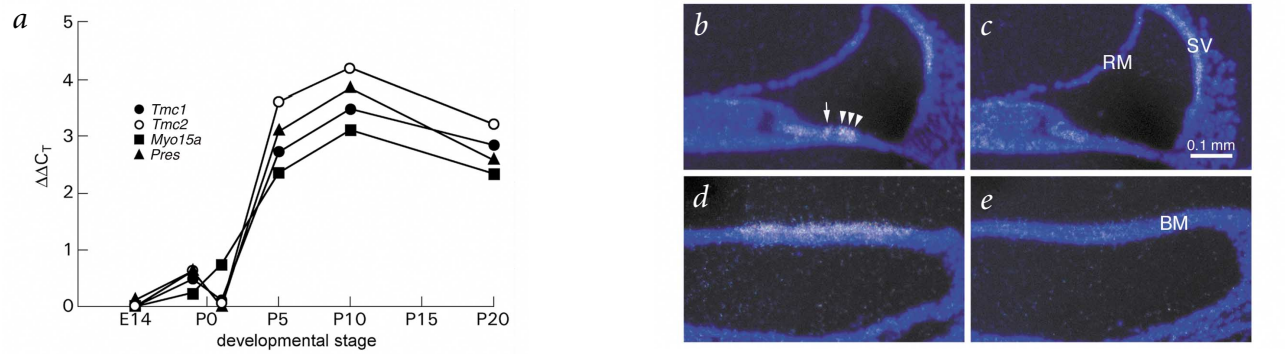

Fig. 6 *Tmc1* mRNA expression in mouse inner ear. ***a***, Real-time quantitative RT–PCR analysis of *Tmc1*, *Tmc2*, *Myo15a* and *Pres* mRNA levels in C57BL/6J mouse temporal bones at E14, E18, P1, P5, P10 and P20. C_T is the observed threshold number of PCR cycles required for detection of the amplification product; ΔC_T is the calculated difference in C_T between the test gene (*Tmc1*, *Tmc2*, *Myo15a* or *Pres*) and an internal control standard (*Gapdh*) measured in the same sample. $\Delta\Delta C_T$ is the calculated difference in ΔC_T between the experimental and E14 time points. *Pres* encodes prestin, a putative outer hair cell motor protein. The increase of *Tmc1* mRNA levels after P1 is consistent with the observed time course of *Tmc1* expression in hair cells as determined by *in situ* hybridization[25]. ***b*–*e***, *In situ* hybridization analysis of *Tmc1* with basal turn of P5 mouse cochlea. Midmodiolar (*b*,*c*) and oblique (*d*,*e*) sections through the organ of Corti were hybridized with antisense (*b*,*d*) and sense (*c*,*e*) cRNA transcripts of the 3′ UTR of *Tmc1*. Sections were counterstained with Hoechst 33258 fluorescent dye to show cell nuclei and photographed in dark field. The antisense *Tmc1* probe specifically hybridizes to inner and outer hair cells (indicated by an arrow and arrowheads in *b*, respectively). RM, Reissner membrane; SV, stria vascularis; BM, basilar membrane.

2.5–3 kb in testis RNA, whereas no hybridization was observed on the same blot probed with the 3′ UTR of *Tmc2* (data not shown).

We assayed the developmental levels of *Tmc1* and *Tmc2* mRNA expression with TaqMan probes by real-time quantitative RT–PCR of total temporal bone RNA from E14, E18, P1, P5, P10 and P20 C57BL/6J control mice. Comparison to levels of internal control *Gapdh* mRNA revealed low, constant levels of *Tmc1* and *Tmc2* mRNA at E14, E18, and P1, which increase by 8–16-fold at P5, P10 and P20 (Fig. 6). We observed similar mRNA levels for *Pres* and *Myo15a*, two other genes expressed specifically in hair cells of the postnatal mouse cochlea[21–23].

We further analyzed *Tmc1* mRNA expression in postnatal (P5) C57BL/6J mouse inner ears. Figure 6*b–e* shows a representative result of three analyses in which the antisense probe (Fig. 6*b*,*d*) specifically hybridized to inner and outer hair cells of the cochlea as well as to neurosensory epithelia of the vestibular end organs (data not shown).

Discussion

***TMC1* mutations cause hearing loss**. The identification of multiple mutations distributed along the entire length of *TMC1* provides evidence of its causative role in deafness. The DFNA36 missense mutation D572N probably acts through a dominant-negative or a gain-of-function mechanism, as at least some of the recessive DFNB7/B11 mutations seem to be functional null alleles yet do not cause hearing loss in heterozygous carriers. The pathogenic nature of IVS13_IVS14del1.6kb in *dn* mice is indicated by the presence of exon 14 in all of the wildtype *Tmc1* cDNA sequences that were cloned (data not shown). Although a previously reported inversion on chromosome 19 (ref. 24) may be a benign rearrangement in linkage dysequilibrium with *dn*, we cannot exclude an additional effect of this inversion upon expression of *Tmc1* in the inner ear or upon expression of other genes on chromosome 19. In addition, the mouse mutation Beethoven (*Bth*) on chromosome 19 is a missense mutation of a conserved methionine residue (M412) of Tmc1 (Fig. 3)[25], indicating that dominant and recessive mutations of *TMC1* can cause progressive postlingual hearing loss and profound prelingual deafness, respectively, in both humans and mice.

A model of six membrane-spanning regions and cytoplasmic N and C termini predicted by TMHMM2.0 indicates that the D572N and *Bth* (M412K) mutations occur in cytoplasmic and extracellular loops, respectively, whereas the recessive missense mutation M654V segregating in family IN-M17 is located in a predicted transmembrane domain. This predicted model of TMC1 membrane topology is similar to those observed in ion channels or transporters, especially the superfamily of multimeric cation channels with six transmembrane segments[26]. M654V may act as a functional null allele by disrupting folding, trafficking, or assembly of its mutant allele products into multimers, whereas D572N and M412K polypeptides may normally fold and assemble with wildtype allele products to exert a dominant negative effect upon the activity of the resulting complex. $Tmc1^{dn}$ encodes a potential translation product with 57 amino acids deleted from the second cytoplasmic loop predicted by TMHMM2.0 and thus may not necessarily comprise a functional null allele. Differences in otoacoustic emissions among normal-hearing heterozygous $Tmc1^{dn/+}$ mice[1] and wildtype controls[27] might reflect a slight dominant effect of $Tmc1^{dn}$. Functional analyses of *TMC1* mutant allele products and identification of additional mutations may test this model.

Mutations in *TMC1* at the DFNB7/B11 locus are a common cause of nonsyndromic recessive deafness in Pakistan and India, where they account for the deafness phenotype in 5.4 ± 3.0% (95% c.i.) of the 230 families that we screened from these areas. The identification of *TMC1* mutations in at least 10 of 11 families segregating deafness linked to this locus on chromosome 9q13–21 suggests that locus heterogeneity is unlikely. The mutations detected in these ten families included nonsense, genomic deletion, splice-site and frameshift mutations that would clearly disrupt the expression or function of *TMC1*. The observed splice acceptor–site substitution in the eleventh family (PKSR25) may be a benign polymorphism in linkage disequilibrium with a mutation in another gene or in a regulatory region of *TMC1*, although this substitution was not observed in 332 control chromosomes. Analyses of nonsyndromic deafness probands from additional ethnic groups should define the contribution of *TMC1* mutations to nonsydromic hearing loss at the DFNA36 and DFNB7/B11 loci in other populations.

The mutant *TMC1/Tmc1* phenotypes of DFNA36, DFNB7/B11 (ref. 12), *dn* (ref. 28) and *Bth* (ref. 25) do not seem to be associated with abnormal vestibular phenotypes, although *Tmc1* mRNA is expressed in the vestibular neuroepithelium. Normal vestibular function has been reported for some recessive deafness phenotypes caused by mutations in genes expressed in both vestibular and auditory end organs[9,11]. The lack of detectable vestibular dysfunction associated with *TMC1* or *Tmc1* mutant phenotypes may reflect basic physiologic differences among the vestibular and auditory systems or functional redundancy with other genes (such as *TMC2/Tmc2*) in the vestibular system.

***TMC2* and *Tmc2* as candidate genes for auditory phenotypic loci.** The identification of *TMC2* and *Tmc2* mRNA transcripts in the inner ear suggests that they may also be crucial for normal auditory function. The functional relationship between *TMC1* and *TMC2* in the auditory and vestibular systems is unknown, but may be elucidated by immunolocalization studies and phenotypic analyses of mouse strains segregating mutant alleles of these genes (such as *Bth*). Although there are no reports of hearing loss loci that co-localize with *TMC2* on human chromosome 20p13, there is an auditory phenotypic candidate locus for *Tmc2* in the region of conserved linkage on mouse chromosome 2. Tailchaser (*Tlc*) is an ENU-induced dominant mutation causing progressive hearing loss and vestibular dysfunction[29]. It is possible that mutations in other *TMC/Tmc* gene family members may also underlie hereditary disorders of balance or hearing.

TMC1 and Tmc1 predicted protein structures. The identification of in-frame stop codons in the 5′ UTRs of *TMC1* and *Tmc1* indicate that the full-length ORFs have indeed been cloned. The sequences adjacent to the first methionine (M1) codons are predicted to be adequate for translation initiation[15]. The next in-frame methionine codon (M113, *TMC1*) is downstream of the R34X, 295delA, and genomic-deletion (exons 4 and 5) mutations, indicating that either M1 is used for translation initiation or these three mutations disrupt mRNA processing, stability or translation efficiency.

The N- and C-terminal regions of TMC1 have a high proportion of charged residues. Sequences with low complexity that are enriched in arginine, lysine, glutamatic acid and proline residues are observed in protein structures with intrinsic disorder[30], indicating that these regions of TMC1 are unlikely to be tightly folded into a single, stable conformation. The distinct clusters of alternating opposite charge in the N terminus suggest a model in which electrostatic interactions mediate the reversible association of adjacent clusters into a structure resembling an accordion or spring. Alternatively, these interactions may mediate the association of the entire domain with a similar domain on another polypeptide (such as TMC1). Testing these models and others will be facilitated by correlation with the function and location of TMC1 in cochlear hair cells.

Possible function of *TMC1* in hair cells. Homozygous *dn* mice are profoundly deaf and never show any measurable electrophysiologic responses to auditory stimuli, although endocochlear potentials are intact[1] and stereocilia may initially appear normal[2]. In contrast to other deaf mouse mutants that either don't develop normal hair cells or stereocilia, or at least show some response to auditory stimuli, the lack of auditory responses in *dn* mice implies a physiologic, not structural, defect of *dn* hair cells. Although subtle ultrastructural abnormalities have been reported for newborn $Tmc1^{dn/dn}$ hair cells[31], the most significant histologic change is degeneration of inner and outer hair cells in the postnatal period[2]. This is consistent with the observed expression of *Tmc1* mRNA in postnatal inner and outer hair cells (Fig. 6). The relative sparing of outer–hair cell stereocilia degeneration in $Tmc1^{Bth/Bth}$ mice[25] does not reflect a lack of *Tmc1* expression in outer hair cells, but may reflect differences in expression of a gene whose product interacts with $Tmc1^{Bth}$.

The distinct auditory phenotypes associated with the *dn* and *Bth* alleles of *Tmc1* (ref. 25), the specific expression of *Tmc1* mRNA in hair cells, the increase of *Tmc1* mRNA levels prior to the onset of auditory function at P12 (Fig. 6) and the prediction of six transmembrane domains indicate that *TMC1* encodes a transmembrane protein that is required for the normal function of cochlear hair cells. It is possible that TMC1, TMC2 or other related proteins mediate an ion-transport or channel function in hair cells, such as the extensively studied mechanotransduction channel activity[32] whose molecular identity remains unknown[5]. We anticipate that determining the *in vivo* functions of *TMC* genes may be difficult, but will be facilitated by immunolocalization and electrophysiology studies and characterization of mice segregating mutant alleles of these genes.

Methods

Ascertainment of human subjects. We obtained approval for this study from institutional review boards (IRBs) at the National Institutes of Health (NINDS/NIDCD joint IRB), Center of Excellence in Molecular Biology (Lahore, Pakistan), All-India Institute of Medical Sciences (Delhi) and the Joint Baycrest Centre/University of Toronto IRB. We obtained informed consent from all study subjects. Consanguineous families segregating autosomal recessive, severe-to-profound, prelingual deafness were ascertained in Pakistan and India. A medical history interview and physical examination of members of the North American LMG128 family were performed by an otolaryngologist (A.J.G.). The ethnicity of LMG128 is unspecified owing to privacy concerns. We assessed vestibular function through a motor developmental history interview and tandem gait and Romberg testing. We carried out pure-tone air conduction audiometry under quiet ambient-noise conditions.

Genotype and linkage analysis. We carried out genomic DNA preparations and genotype analyses as described[9]. Samples from affected individuals of Indian and Pakistani families with three or more affected individuals were screened for homozygosity for markers linked to known DFNB loci, and linkage calculations for DFNB7/B11 families were carried out as described[9]. We carried out linkage analysis of the DFNA36 family LMG128 essentially as described[9], but with the phenotype set as autosomal dominant with penetrance equal to 0.99, disease-allele frequency of 0.0001, equal marker allele frequencies of 0.1, and a phenocopy rate of 1/1,000.

RACE-ready inner-ear cDNA libraries. We used the Micro-Fast Track Kit (Invitrogen) to isolate poly(A+) RNA from human fetal cochleae at 17.5–23 wk or BALB/c mouse cochleae at 14 d. We prepared cochlear RACE-ready cDNA with the Marathon cDNA Amplification Kit (Clontech). RACE-ready cDNA libraries derived from E17 mouse embryo, mouse fetal brain, human brain, human fetal brain and human placenta were purchased from Clontech.

RT–PCR and RACE analyses: *TMC1*. We used genomic *TMC1* sequence to design primers HcDNAF#15 and HcDNAR#11 for PCR amplification of *TMC1* from human inner-ear, fetal brain and placenta cDNA libraries. Amplifications were carried out in 50-μl reaction volumes with cDNA Advantage Polymerase (Clontech) and cycling conditions recommended by the manufacturer. We used the sequence of the 0.8-kb product to design primers H5RACE#1 and H5RACE#2 for 5′ RACE of RACE-ready human placenta cDNA (Clontech). Upstream primers H5RACE#3 and H5RACE#4 were thus designed for a second round of 5′ RACE. GENSCAN analysis of human genomic DNA and comparison to the 3′ UTR of mouse *Tmc1* was used to identify exon 24 encoding the 3′ end of *TMC1*. We used reverse primer Hnp2/3′R2, corresponding to the predicted 3′ UTR, and forward primer 3UTR#3 to amplify the 3′ end of *TMC1* from the human placenta cDNA library. cDNA encoding the entire *TMC1* ORF was amplified and sequenced from the human placental cDNA library using primers HcDNAF#9 and HcDNAR#18. Primer sequences are available from the corresponding author upon request.

RT–PCR and RACE analyses: *Tmc1*. EST database queries for sequence similarity to *TMC1* identified mouse IMAGE cDNA clone 602169, which was purchased from Research Genetics. The sequence analysis of IMAGE:602169 was confirmed and completed in order to design 5′-RACE primers M5RACE#1 and M5RACE#2 and 3′-RACE primers M3RACE#1 and M3RACE#2. RACE substrates were RACE-ready cDNA libraries derived from mouse cochlea, fetal brain and E17 whole embryos. We amplified and sequenced the complete *Tmc1* ORF with primers McDNAF#4 and McDNAR#13 from a mouse organ of Corti cell line, UB/OC-1 (ref. 33) and E17 mouse embryo RACE-ready cDNA.

RT–PCR and RACE analyses: *TMC2* and *Tmc2*. We used conserved sequences among *TMC1*, *Tmc1* and potential exons of *TMC2* and *Tmc2* to design PCR primers TDC2-7F and TDC2-8R for amplification and sequencing of a 187-bp *Tmc2* cDNA (spanning two exons) from the mouse inner-ear cDNA library. We used the resulting sequence to design a first set of primers for sequential 5′- and 3′-RACE analyses of the mouse testis cDNA library. We used the RACE product sequences to design primer sets Tdc2-F2/Tdc2-7RR and Tdc2-7L/Tdc2-R2 for PCR amplification of two overlapping cDNA fragments spanning the complete *Tmc2* ORF. Sequence conservation among *Tmc2* and human genomic sequence was used to design primer sets TDC2-F2/TDC2-5R and TDC2-4L/TDC2-R2 for amplification of two overlapping *TMC2* cDNA fragments from a human brain cDNA library.

***TMC1* and *Tmc1* mutation analyses.** We determined the genomic structures of *TMC1* and *Tmc1* by alignment of cDNA sequences with high-throughput genome sequence (htgs) data, as well as *TMC1* genomic sequence from the Celera Publication site[34] and *Tmc1* genomic sequence data generated through the use of the Celera Discovery System and Celera's associated databases. We amplified *TMC1* exons from genomic DNA and sequenced them as previously described with intronic primers flanking *TMC1* exons[9]. We obtained panethnic and Caucasian diversity panels of DNA samples from the NIGMS Human Genetic Cell Repository (Coriell Cell Repositories). We amplified and sequenced *Tmc1* exons with flanking intronic primers. Control samples included parental curly-tail (*ct/ct*) strain DNA and 129/J, AKR/J, BALB/cJ, C3H/HeJ, C57BL/6J, C58/J, CBA/J, CE/J, DBA/2J, P/J, RF/J, SEA/GnJ and SWR/J DNA samples that were purchased from The Jackson Laboratories. We identified the IVS13_IVS14del1.6kb mutation by PCR amplification and sequencing of *dn* genomic DNA with primers Ex14F and IVS14-1R. We determined the deletion breakpoint sites in wildtype genomic DNA by amplification and sequencing with primers KF and Ex14R for the upstream breakpoint site and primers IVS14-1L and IVS14-1R for the downstream breakpoint site.

Real-time quantitative RT–PCR. We dissected temporal bones from C57BL/6J mice at E14, E18, P1, P5, P10 and P20. We prepared total RNA from each time point from 12 pooled temporal bones in cell lysis buffer (RNeasy Mini Kit, Qiagen), using an FP120 FastPrep Cell Disruptor (Bio101) at 6.5 m s^{-1} for 45 s. RNA was reverse-transcribed with the SuperScript Preamplification System for First Strand cDNA Synthesis (Life Technology). We carried out real-time PCR with TaqMan Universal PCR master mix and an ABI Prism 7700 (both from Applied Biosystems). We designed primers and probes with Primer Express v. 1.0 (Applied Biosystems). We obtained TaqMan probes and *GAPDH* control primers from Applied Biosystems (Taqman Rodent GAPDH Control Reagents, VIC Probe).

***In situ* hybridization analyses.** We subcloned cDNA encoding the 3′ UTR of *Tmc1* (nt 2466–2895) into pGEM-T Easy (Promega) and confirmed cDNA insert orientations by sequence analysis. The *Tmc1* probe has no sequence similarity with *Tmc2* or any other sequences in publicly available databases. We generated cRNA probes with T7 RNA polymerase in the presence of [α-^{35}S]UTP. We processed C57BL/6J mouse temporal bones essentially as described[35,36]. Sagittally dissected hemi-heads from P5 mice were fixed overnight in PBS / 4% paraformaldehyde and mounted in paraffin. Radiolabeled cRNA probes were hybridized with 10-μm transverse sections and detected by autoradiography.

GenBank accession numbers. Human *TMC1* cDNA, AF417578; mouse *Tmc1* cDNA, AF417579; human *TMC2* cDNA, AF417580; mouse *Tmc2* cDNA, AF417581.

Acknowledgments

We thank the study families for their participation, L. Davis, S.S. Ng, and B. Ploplis for technical assistance; D. Wu, T. Picton, R. Morell, M. Kelley, S. Vreugde and P. Lanford for assistance and advice; C. Morton for providing human fetal cochlear RNA; and P. Steinbach and members of the LMG for helpful discussions. This research was supported by NIDCD/NIH intramural funds from the National Institutes of Health–National Institute on Deafness and Other Communication Disorders (to J.F.B., T.B.F. and A.J.G.).

Competing interests statement

Some authors declare competing financial interests (T.B.F., E.R.W. and A.J.G.). Details accompany the paper on the website of Nature Genetics (http://genetics.nature.com).

Received 5 November; accepted 16 January 2002.

1. Steel, K.P. & Bock, G.R. The nature of inherited deafness in *deafness* mice. *Nature* **288**, 159–161 (1980).
2. Bock, G.R. & Steel, K.P. Inner ear pathology in the deafness mutant mouse. *Acta Otolaryngol.* **96**, 39–47 (1983).
3. Ashmore, J.F. & Mammano, F. Can you still see the cochlea for the molecules? *Curr. Opin. Neurobiol.* **11**, 449–454 (2001).
4. Griffith, A.J. & Friedman, T.B. Making sense out of sound. *Nature Genet.* **21**, 347–349 (1999).
5. Gillespie, P.G. & Walker, R.G. Molecular basis of mechanosensory transduction. *Nature* **413**, 194–202 (2001).
6. Ahmed, Z.M. *et al.* Mutations of the protocadherin gene *PCDH15* cause Usher syndrome type 1F. *Am. J. Hum. Genet.* **69**, 25–34 (2001).
7. Alagramam, K.N. *et al.* The mouse Ames waltzer hearing-loss mutant is caused by mutation of *Pcdh15*, a novel protocadherin gene. *Nature Genet.* **27**, 99–102 (2001).
8. Bolz, H. *et al.* Mutation of *CDH23*, encoding a new member of the cadherin gene family, causes Usher syndrome type 1D. *Nature Genet.* **27**, 108–112 (2001).
9. Bork, J.M. *et al.* Usher syndrome 1D and nonsyndromic autosomal recessive deafness DFNB12 are caused by allelic mutations of the novel cadherin-like gene *CDH23*. *Am. J. Hum. Genet.* **68**, 26–37 (2001).
10. Verpy, E. *et al.* Mutations in a new gene encoding a protein of the hair bundle cause non-syndromic deafness at the DFNB16 locus. *Nature Genet.* **29**, 345–349 (2001).
11. Wilcox, E.R. *et al.* Mutations in the gene encoding tight junction claudin-14 cause autosomal recessive deafness DFNB29. *Cell* **104**, 165–172 (2001).
12. Jain, P.K. *et al.* A human recessive neurosensory nonsyndromic hearing impairment locus is potential homologue of murine deafness (*dn*) locus. *Hum. Mol. Genet.* **4**, 2391–2394 (1995).
13. Scott, D.A. *et al.* An autosomal recessive nonsyndromic-hearing-loss locus identified by DNA pooling using two inbred Bedouin kindreds. *Am. J. Hum. Genet.* **59**, 385–391 (1996).
14. Scott, D.A. *et al.* Refining the DFNB7-DFNB11 deafness locus using intragenic polymorphisms in a novel gene, *TMEM2*. *Gene* **246**, 265–274 (2000).
15. Suzuki, Y. *et al.* Statistical analysis of the 5′ untranslated region of human mRNA using "Oligo-Capped" cDNA libraries. *Genomics* **64**, 286–297 (2000).
16. Kozak, M. Compilation and analysis of sequences upstream from the translational start site in eukaryotic mRNAs. *Nucleic Acids Res.* **12**, 857–872 (1984).
17. Thompson, J.D., Higgins, D.G. & Gibson, T.J. CLUSTAL W: improving the sensitivity of progressive multiple sequence alignment through sequence weighting, position-specific gap penalties and weight matrix choice. *Nucleic Acids Res.* **22**, 4673–4680 (1994).
18. Keats, B.J. *et al.* The deafness locus (*dn*) maps to mouse chromosome 19. *Mamm. Genome* **6**, 8–10 (1995).
19. Moller, S., Croning, M.D. & Apweiler, R. Evaluation of methods for the prediction of membrane spanning regions. *Bioinformatics* **17**, 646–653 (2001).
20. Nielsen, H., Engelbrecht, J., Brunak, S. & von Heijne, G. Identification of prokaryotic and eukaryotic signal peptides and prediction of their cleavage sites. *Protein Eng.* **10**, 1–6 (1997).
21. Wang, A. *et al.* Association of unconventional myosin *MYO15* mutations with human nonsyndromic deafness DFNB3. *Science* **280**, 1447–1451 (1998).
22. Liang, Y. *et al.* Characterization of the human and mouse unconventional myosin XV genes responsible for hereditary deafness *DFNB3* and shaker 2. *Genomics* **61**, 243–258 (1999).
23. Belyantseva, I.A., Adler, H.J., Curi, R., Frolenkov, G.I. & Kachar, B. Expression and localization of prestin and the sugar transporter GLUT-5 during development of electromotility in cochlear outer hair cells. *J. Neurosci.* **20**, RC116 (2000).
24. Vinas, A.M. *et al.* The mouse deafness locus (*dn*) is associated with an inversion on chromosome 19. *Biochim. Biophys. Acta* **1407**, 257–262 (1998).
25. Vreugde, S. *et al.* Beethoven, a mouse model for dominant progressive hearing loss DFNA36. *Nature Genet.*, **30**, 257–258 (2002).
26. Clapham, D.E., Runnels, L.W. & Strübing, C. The TRP ion channel family. *Nature Rev. Neurosci*. **2**, 387–396 (2001).
27. Huang, J.M., Berlin, C.I., Lin, S.T. & Keats, B.J. Low intensities and 1.3 ratio produce distortion product otoacoustic emissions which are larger in heterozygous (+/*dn*) than homozygous (+/+) mice. *Hear. Res.* **117**, 24–30 (1998).
28. Deol, M.S. & Kocher, W. A new gene for deafness in the mouse. *Heredity* **12**, 463–466 (1958).
29. Kiernan, A.E. *et al.* Tailchaser (*Tlc*): a new mouse mutation affecting hair bundle differentiation and hair cell survival. *J. Neurocytol.* **28**, 969–985 (1999).
30. Romero, P. *et al.* Sequence complexity of disordered protein. *Proteins* **42**, 38–48 (2001).
31. Pujol, R., Shnerson, A., Lenoir, M. & Deol, M.S. Early degeneration of sensory and ganglion cells in the inner ear of mice with uncomplicated genetic deafness (*dn*): preliminary observations. *Hear. Res.* **12**, 57–63 (1983).
32. Hudspeth, A.J. & Corey, D.P. Sensitivity, polarity, and conductance change in the response of vertebrate hair cells to controlled mechanical stimuli. *Proc. Natl Acad. Sci. U S A* **74**, 2407–2411 (1977).
33. Rivolta, M.N. *et al.* Auditory hair cell precursors immortalized from the mammalian inner ear. *Proc. R. Soc. Lond. B Biol. Sci.* **265**, 1595–1603 (1998).
34. Venter, J.C. *et al.* The sequence of the human genome. *Science* **291**, 1304–1351 (2001).
35. Ressler, K.J., Sullivan, S.L. & Buck, L.B. Information coding in the olfactory system: evidence for a stereotyped and highly organized epitope map in the olfactory bulb. *Cell* **79**, 1245–1255 (1994).
36. Sassoon, D.A., Garner, I. & Buckingham, M. Transcripts of alpha-cardiac and alpha-skeletal actins are early markers for myogenesis in the mouse embryo. *Development* **104**, 155–164 (1988).